Research Article

Improved hydrogen storage properties of MgH_2 by the addition of TiCN and its catalytic mechanism

Liuting Zhang[1] · Liang Ji[1] · Zhendong Yao[3] · Zeliang Cai[1] · Ze Sun[1] · Nianhua Yan[1] · Xinqiao Zhu[2]

Abstract

The hydrogen storage properties of MgH_2–x wt%TiCN ($x = 5$, 10, 15) composites were systematically investigated and the results show that the addition of TiCN can effectively improve the de/rehydrogenation kinetics of MgH_2. Taken the onset dehydrogenation temperature and isothermal de/rehydrogenation kinetics into consideration, the MgH_2–10 wt% TiCN composite was shown to have the best performance. It was found that the MgH_2–10 wt% TiCN composite could release 4 wt% H_2 in 17.3 min at 300 °C while the as-synthesized MgH_2 could not release any hydrogen under the same condition. Besides, the MgH_2–10 wt% TiCN composite could absorb 4.63 wt% H_2 under 3.2 MPa hydrogen pressure at 300 °C within 20 s. Compared with as-synthesized MgH_2, the activation energy of the MgH_2–10 wt% TiCN composite was significantly decreased from 183.76 ± 10 to 106.82 ± 5 kJ/mol. X-ray diffraction analysis revealed that the TiCN remained stable during the ball milling and the following de/rehydrogenation cycle. The catalytic mechanism was also proposed that the TiCN particles absorbed on MgH_2 not only served as charge transfer centers and accelerated the hydrogen incorporation and dissociation rate but also provided more diffusion channels for hydrogen, which contributed to the good de/rehydrogenation properties of MgH_2.

Keywords Hydrogen storage · MgH_2–TiCN composites · Kinetics · Catalytic mechanism

1 Introduction

Nowadays, it is urgent to find a cost-effective and renewable energy source to replace fossil fuels for a sustainable and clean world [1]. Among various new energy carriers, hydrogen is one of the most promising candidates as it can be converted to electricity through fuel cell without emitting pollutants [2]. However, the realization of the "hydrogen economy" requires a high energy density and safe hydrogen storage technology [3]. So far, numerous efforts have been made by researchers worldwide to develop hydrogen storage materials to meet the requirements of effective capacity, safety, mild reaction temperature and operating pressure. Magnesium hydride is hopeful to be used as hydrogen storage materials due to its high hydrogen capacity (7.6 wt% and 110 kg/m^3). However, the high thermodynamic stability and slow kinetic properties hinder the practical use of MgH_2 [4, 5]. In recent years, it has been found that adding additives or catalysts to matrixes can reduce the energy of the metal-hydrogen bonds and lower the desorption energy of MgH_2 [6–15]. Sulaiman et al. [16] demonstrated that the onset dehydrogenation temperature of MgH_2 doped with 10 wt% K_2NiF_6 and 5 wt% CNTs could be reduced to 245 °C. Antonio et al.

Liuting Zhang, Liang Ji and Zhendong Yao have contributed equally to this work.

Electronic supplementary material The online version of this article (https://doi.org/10.1007/s42452-018-0093-9) contains supplementary material, which is available to authorized users.

✉ Xinqiao Zhu, zhuxinqiao@zju.edu.cn | [1]School of Energy and Power, Jiangsu University of Science and Technology, Zhenjiang 212003, China. [2]Institute of Nuclear Physics and Chemistry, China Academy of Engineering Physics, Mianyang 621999, China. [3]Department of Materials Science and Engineering, Zhejiang University, Hangzhou 310027, China.

SN Applied Sciences (2019) 1:101 | https://doi.org/10.1007/s42452-018-0093-9

Received: 7 November 2018 / Accepted: 29 November 2018 / Published online: 17 December 2018

[17] revealed that $VNbO_5$ could lower the desorption temperature of MgH_2 from 330 to 235 °C. Yahya et al. [18] reported that the MgH_2–5 wt% K_2NbF_7 composite started to release hydrogen at 255 °C, which was 75 °C lower than the as-milled MgH_2. Ali et al. [19] studied the effect of nanolayer-like-shaped $MgFe_2O_4$ on the performance of MgH_2 for hydrogen storage, the isothermal desorption kinetic study showed that the doped sample could desorb approximately 4.8 wt% H_2 in 10 min while the milled MgH_2 desorbed less than 1.0 wt% H_2 at 320 °C.

Compared with above additives and catalysts, Ti-based materials are superior because of their unique electrical and chemical properties [20–26]. For instance, Zhang et al. [27] found that the MgH_2–10 wt% TiO_2@C sample started releasing hydrogen at 205 °C, which was 95 °C lower than that of pristine MgH_2. Ma et al. [28]. found that the hydrogen absorption of MgH_2 can be largely completed within 25 s at a moderate temperature range (40–100 °C) after adding 4 mol % TiF_3. Pandey et al. [29]. found that the desorption temperature of 50 nm TiO_2 modified MgH_2 was 310 °C, which is 96 °C lower compared to that of commercial MgH_2. Cui et al. [30]. coated a Ti nano-layer on the surface of Mg,which remarkably accelerated the hydrogen dissociation and recombination process. Recently, it has been demonstrated that TiC and TiN can greatly improve the hydrogen storage performances of MgH_2 [31–34]. For instance, Fan et al. [35] found that the MgH_2–10 wt% TiC composite could release 6.3 wt% H_2 at 300 °C and absorb 4.1 wt% H_2 under 1 MPa at 100 °C. Wang et al. [36] successfully synthesized TiN@rGO nanocomposites through a simple "urea glass" technique. The MgH_2–10 wt% TiN@rGO composite began to release hydrogen at 167 °C and could release 6.0 wt% H_2 within 18 min at 309 °C.

In this work, the catalytic effect of TiCN on the hydrogen storage properties of MgH_2 was investigated. So far as we know, the hydrogen storage properties of MgH_2–TiCN composites have never been systematically studied before. Here, we use ball milling technology to prepare MgH_2–TiCN composites. The hydrogen absorption and desorption properties of MgH_2–TiCN composites were investigated and its catalytic mechanism was also discussed in detail.

2 Experimental

2.1 Preparation of as-synthesized MgH_2

The MgH_2 used was synthesized by mechanical ball milling and hydrogenation heat treatment. In brief, 6 g Mg powder (Sinopharm Chemical Reagent Co., Ltd, 99%, 100–200 mesh) was hydrogenated at the hydrogen pressure of 65 bar and 380 °C for 2 h. Then the power was divided into two parts and milled at 450 rpm for 5 h. Repeat the above steps and MgH_2 can be obtained after finally hydrogenate the power at the hydrogen pressure of 65 bar and 380 °C for 2 h.

2.2 Preparation of MgH_2–TiCN composites

The TiCN (aladdin, 1–2 μm, 99%) and the as-synthesized MgH_2 (0.5–2 μm, shown in Fig. S1) were mixed with a mass ratio of 5:95, 10:90, and 15:85, respectively. The mixtures were then ball milled at a speed of 450 rpm for 2 h under 0.1 MPa argon atmosphere. The ball to material ratio was 40:1. To avoid contamination, all the samples handling and transferring were carried out in an Ar-filled glove box (Mikrouna) with a water/oxygen content of less than 1 ppm.

2.3 Characterization

XRD tests of the samples were performed on an X'Pert Pro X-ray diffractometer (PANalytical, the Netherlands) with Cu K alpha radiation at 40 kV, 40 mA. During transferring and scanning, a home-made argon-filled device was adopted to avoid oxygen and moisture contamination. The morphology and elemental distribution of the samples were further analyzed using a scanning electron microscope (SEM, Hitachi SU-70, 3.0 kV) equipped with an X-ray energy spectrometer (EDX, HORIBAX-MAX). The DSC curve was carried out on an analyzer model (Netzsch STA449F3) with flowing argon (99.999%, 50 mL/min) as protective gas. The quantitative de/rehydrogenation properties of the as-synthesized MgH_2 and as-prepared MgH_2–5 wt% TiCN, MgH_2–10 wt% TiCN, MgH_2–15 wt% TiCN composites were measured with a Sieverts apparatus. Dehydrogenation was carried out at a temperature of 275, 300 and 325 °C under a hydrogen pressure of 3 kpa, respectively. Rehydrogenation was performed at a temperature of 200, 250 and 300 °C under an initial hydrogen pressure of 3.2 MPa, respectively. It is worth noting that the hydrogen capacity is given in weight percent of the entire composite including the additives.

3 Results and discussion

In order to study the effect of TiCN on the hydrogen storage performance of MgH_2, various amount of TiCN were added to MgH_2 by ball milling. Figure 1 shows the XRD patterns of as-synthesized MgH_2, commercial TiCN, as-prepared MgH_2–5 wt% TiCN, MgH_2–10 wt% TiCN, and MgH_2–15 wt% TiCN, respectively. Just as commercial MgH_2 [37], weak signal of Mg phase can be seen from Fig. 1a, indicating the impurity of as-synthesized MgH_2. After TiCN was introduced, TiCN can be easily distinguished

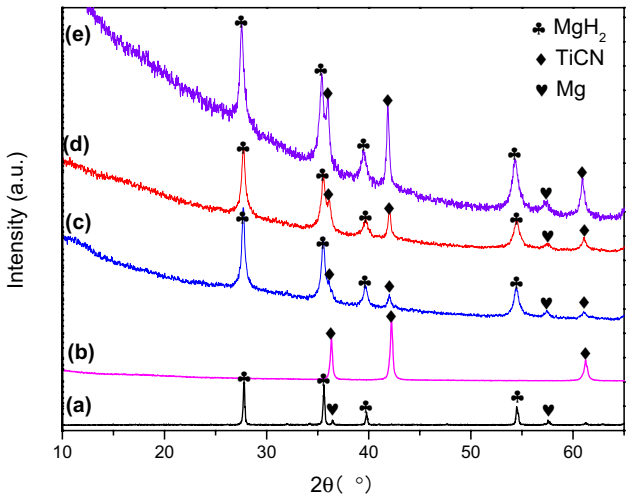

Fig. 1 XRD patterns of **a** as-synthesized MgH_2, **b** bulk TiCN, **c** as-prepared MgH_2–5 wt% TiCN, **d** MgH_2–10 wt% TiCN and **e** MgH_2–15 wt% TiCN

from Fig. 1c, d and e and the signal of TiCN phase became stronger with its increasing weight percent. From the XRD analysis, no new phases can be observed in the ball milled composites, indicating the as-prepared MgH_2–TiCN composites are just physical mixtures.

The morphology of as-synthesized MgH_2, as-prepared MgH_2–5 wt% TiCN, MgH_2–10 wt% TiCN and MgH_2–15 wt% TiCN composites were investigated by SEM measurement. As can be seen from Fig. S1 that the particle sizes of TiCN are in micron scales. Most of the particles are ca. 2 um in size, and many small particles of 1 um aggregate around these large particles. It can be observed from Fig. 2 and that there was no obvious change in the size of MgH_2 after the addition of TiCN, and many small particles absorbed on MgH_2 after ball milling.

As shown in Fig. 3, the dehydrogenation performance of as-prepared MgH_2–TiCN composites were firstly investigated by differential scanning calorimetry (DSC) measurement at a heating rate of 5 °C/min under flowing Ar condition. For comparison, the DSC curves of commercial MgH_2 and as-synthesized MgH_2 were also presented. Commercial MgH_2 started to decompose at 405.9 °C with a peak temperature of 420 °C. The as-synthesized MgH_2 shows a lower onset dehydrogenation and peak temperature of 322.0 °C and 353.5 °C, which was caused by the ball milling effect during the synthesize process [38]. It is noteworthy that both the onset dehydrogenation temperature and

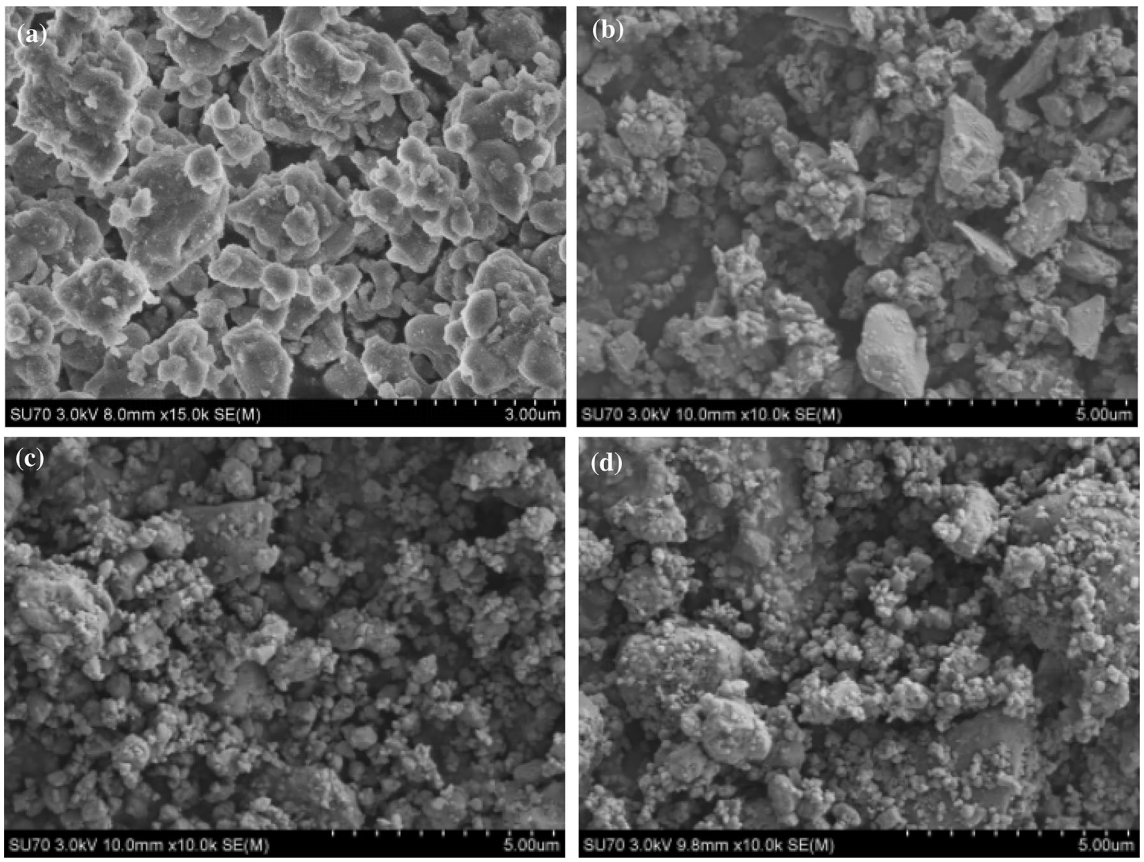

Fig. 2 SEM images of **a** as-synthesized MgH_2, **b** as-prepared MgH_2–5 wt% TiCN, **c** MgH_2–10 wt% TiCN and **d** MgH_2–15 wt% TiCN

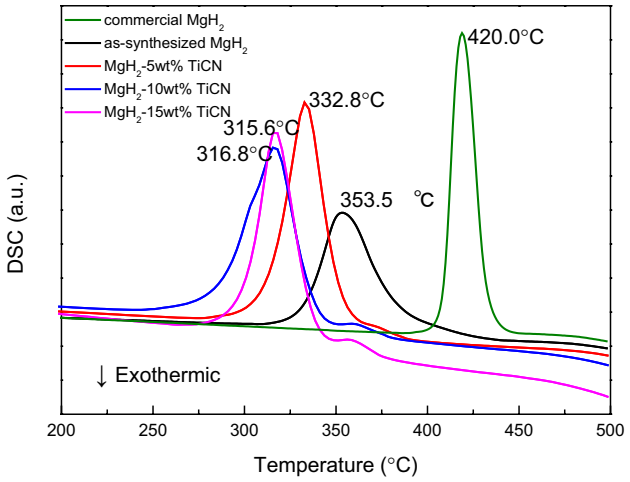

Fig. 3 DSC curves of commercial MgH_2, as-synthesized MgH_2, as-prepared MgH_2–5 wt% TiCN, MgH_2–10 wt% TiCN, and MgH_2–15 wt% TiCN composites

Table 1 The operating temperatures of different samples from DSC

Sample	Initial temperature (°C)	Peak temperature (°C)
Commercial MgH_2	405.9	420.0
As-synthesized MgH_2	322.0	353.5
MgH_2–5 wt% TiCN	298.4	332.8
MgH_2–10 wt% TiCN	280.9	316.8
MgH_2–15 wt% TiCN	278.5	315.6

the peak temperature of MgH_2–TiCN composites are significantly reduced by the addition of different amount of TiCN (see Table 1 for details). The onset dehydrogenation temperature and peak temperature of MgH_2–5 wt% TiCN and MgH_2–10 wt% TiCN composites are 298.4 °C, 280.9 °C and 332.8 °C, 316.8 °C, respectively, which are lower than that of commercial MgH_2 by around 100 °C. Compared with MgH_2–10 wt% TiCN, the onset dehydrogenation temperature and peak temperature of MgH_2–15 wt% TiCN are almost the same. As shown by the DSC curves, the dehydrogenation temperature of the MgH_2–10 wt% TiCN composite material is significantly reduced, indicating that the addition of 10 wt% TiCN has an excellent catalytic effect and its performance is superior to that of MgH_2–5 wt% TiCN. Further increase the amount of TiCN to 15 wt%, the catalytic effect of TiCN on MgH_2 has not been significantly improved.

To compare the hydrogen desorption kinetics of 5 wt% TiCN, 10 wt% TiCN and 15 wt% TiCN modified MgH_2, isothermal dehydrogenation tests were conducted at 275, 300 and 325 °C, respectively. Figure 4 displays the dehydrogenation kinetics of as-synthesized MgH_2, as-prepared MgH_2–5 wt% TiCN, MgH_2–10 wt% TiCN and MgH_2–15 wt% TiCN composites, respectively. It can be seen from Fig. 4a that the as-synthesized MgH_2 could not release any hydrogen at 275 °C while the addition of TiCN can significantly improve the hydrogen release kinetics of MgH_2–TiCN composites. The MgH_2–5 wt% TiCN, MgH_2–10 wt% TiCN and MgH_2–15 wt% TiCN composites only need 102.5, 61.8 and 49.3 min to release 4 wt% H_2, respectively. It can be seen from Fig. 4b, with the operation temperature increased to 300 °C, the as-synthesized MgH_2 still did not release any hydrogen, while the time needed to release 4 wt% H_2 for MgH_2–5 wt% TiCN, MgH_2–10 wt% TiCN and MgH_2–15 wt% TiCN composites was decreased to 24.6, 17.3 and 16.3 min, respectively. In Fig. 4c, the as-synthesized MgH_2 started to release a little hydrogen (0.5 wt% H_2 in 43 min) when further increasing the operation temperature to 325 °C. For the MgH_2–5 wt% TiCN, MgH_2–10 wt% TiCN and MgH_2–15 wt% TiCN composites, with an equivalent amount of 4 wt% hydrogen was released, the time taken was 11.8, 8.5, and 7 min, respectively. Obviously, the MgH_2–TiCN composites show faster hydrogen release kinetics with the increasing operation temperature. Comparing the three different MgH_2–TiCN composites, the dehydrogenation kinetics of MgH_2–10 wt% TiCN is superior to that of MgH_2–5 wt% TiCN, but it is similar to that of MgH_2–15 wt% TiCN, which is in consistent with the DSC results. In addition, it can ben seen from Fig. 4 that the total hydrogen capacity decreases with the increasing addition of TiCN. Considering the onset dehydrogenation temperature, dehydrogenation kinetics and the hydrogen capacity, MgH_2–10 wt% TiCN composite was chosen for further investigation.

The isothermal rehydrogenation measurement of the MgH_2–10 wt% TiCN composite after complete dehydrogenation was further carried out under 3.2 MPa hydrogen pressure at 200, 250 and 300 °C, respectively. As well as the improved desorption kinetics, the MgH_2–10 wt%TiCN composite also exhibits enhanced absorption kinetics, as shown in Fig. 5. It is clearly shown in Fig. 5b that the MgH_2–10 wt% TiCN composite could absorb 0.64, 4.16, 4.63 wt% H_2 within 20 s at 200, 250 and 300 °C, respectively, while the as-synthesized MgH_2 could only absorb 2.91 wt% H_2 at 300 °C. From above experimental results, it is verified that the hydrogen storage property of MgH_2 can be remarkably enhanced by the addition of TiCN.

For better understanding the reason of the enhanced dehydrogenation kinetics of the MgH_2–TiCN system, the Kissinger's method was adopted to calculate the activation energy (E_a) via the equation:

$$\ln\left(\beta/T_p^2\right) = -E_a/RT_p + \ln\left(AR/E_a\right)$$

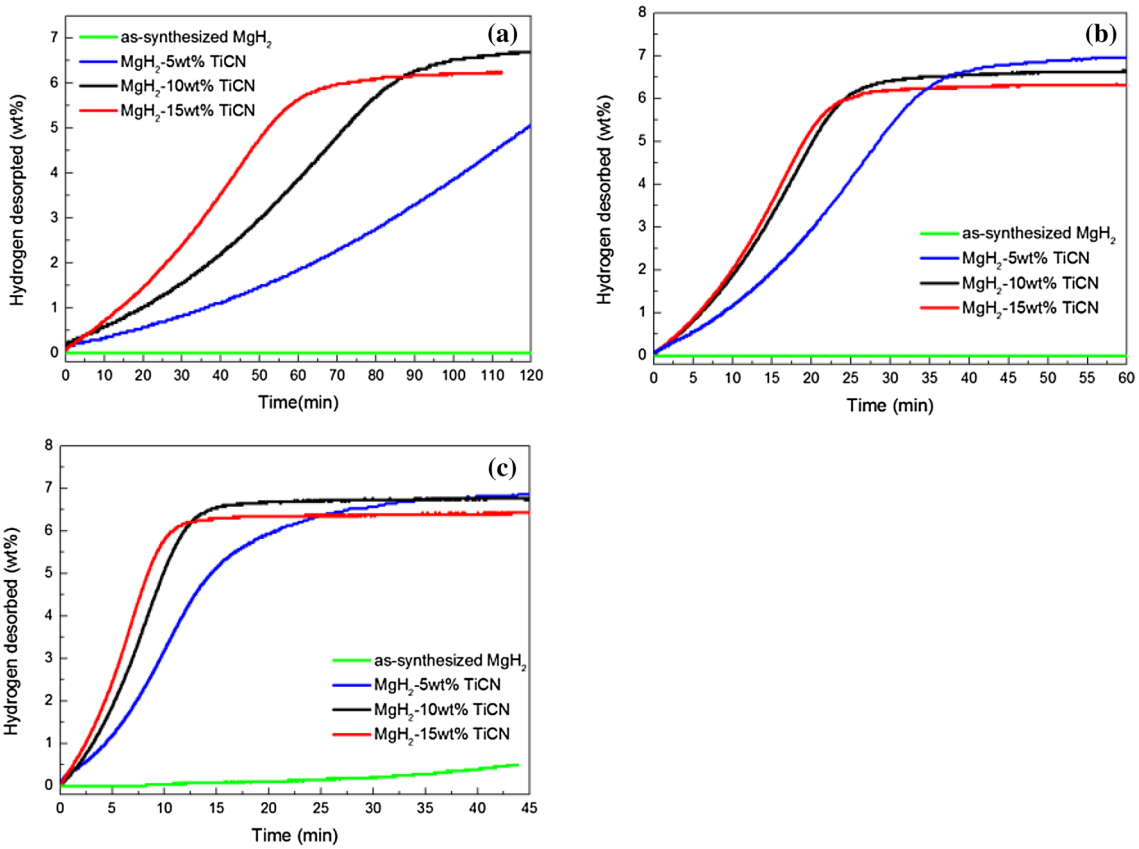

Fig. 4 Isothermal desorption curves of as-synthesized MgH_2, as-prepared MgH_2–5 wt% TiCN, MgH_2–10 wt% TiCN and MgH_2–15 wt% TiCN composites at **a** 275 °C, **b** 300 °C, **c** 325 °C

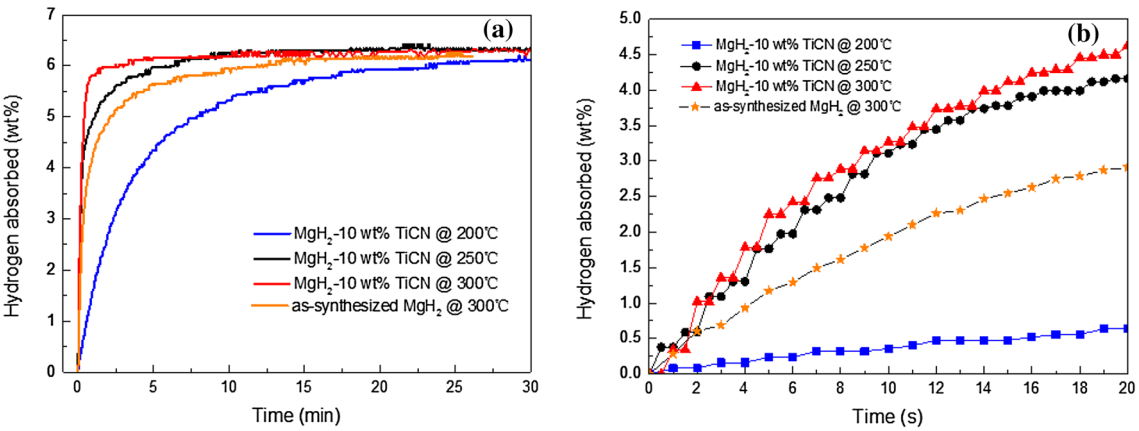

Fig. 5 **a** Isothermal absorption curves of the dehydrogenated sample of MgH_2–10 wt% TiCN at different temperatures under 3.2 MPa hydrogen pressure; **b** the enlarged portion of the first 20 s in (**a**)

where β, T_p, A, and R represents the heating rate, the absolute temperature at the maximum hydrogen evolution rate, the pre-exponential factor and the gas constant, respectively [39]. In this paper, T_p can be obtained from the DSC curves from Fig. 6a and b. Figure 6c shows the dependence of ln (β/T_p^2) on $1/T_p$. The E_a of the as-synthesized MgH_2 is calculated to be 183.76 ± 10 kJ/mol, which is similar to that of commercial MgH_2 [37]. However, the E_a of MgH_2–10 wt% TiCN composite is estimated to be 106.82 ± 5 kJ/mol, which is ca. 77 kJ/mol lower than that of as-synthesized MgH_2. As can be seen from Table 2, compared with other modified MgH_2 system, the

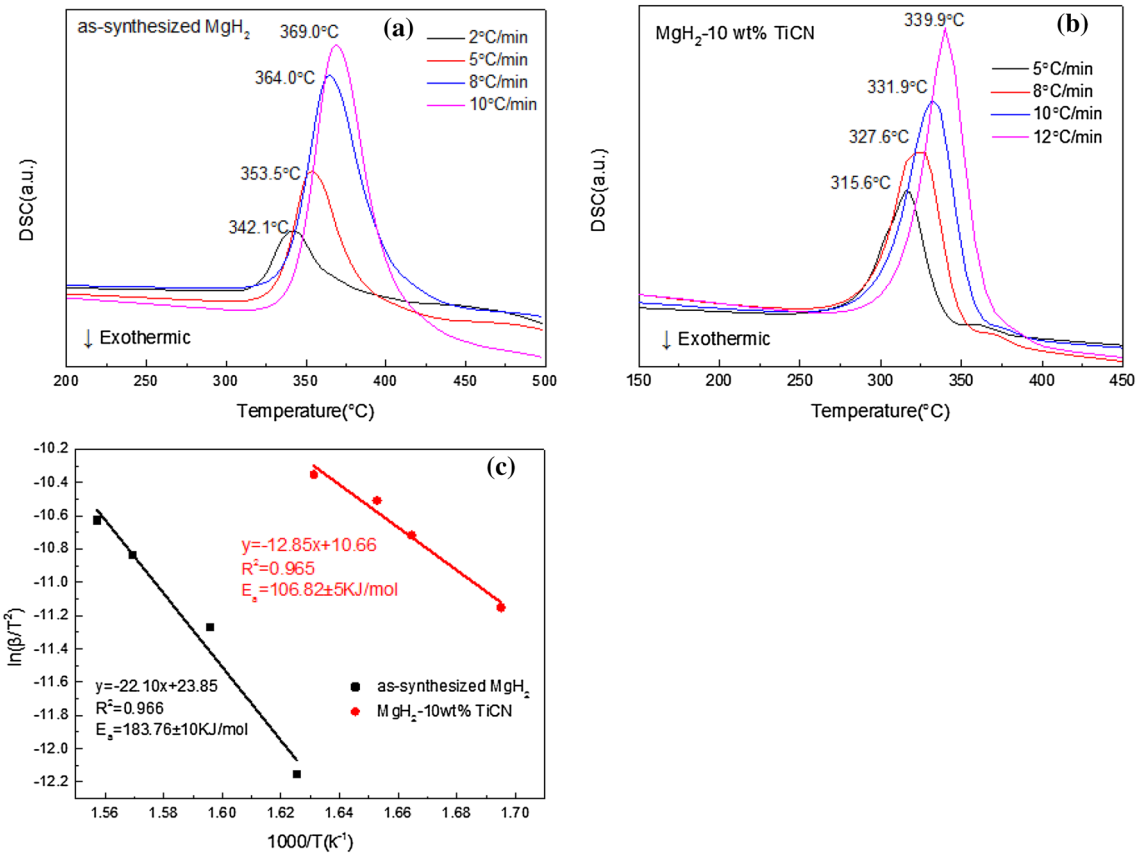

Fig. 6 DSC profiles of **a** as-synthesized MgH_2 for various heating rates (2, 5, 8 and 10 °C/min), **b** MgH_2–10 wt% TiCN for various heating rates (5, 8, 10 and 12 °C/min) and **c** estimation of the apparent activation energies (Ea) using the Kissinger method

Table 2 The apparent activation energy of MgH_2 modified systems

Sample	The apparent activation energy (kJ/mol)	References
MgH_2–Nb_2O_5–MWCNT	141.46	[40]
MgH_2–10 wt% $SrTiO_3$	109	[41]
MgH_2–10 wt% $SrFe_{12}O_{19}$	114.22	[42]
MgH_2–10 wt% $CeCl_3$	149	[43]
MgH_2–10 wt% TiCN	106.82	This work

MgH_2–10 wt% TiCN composite shows the lowest activation energy [40–43], demonstrating the great catalytic effect of TiCN. The remarkable decrease in the activation energy of MgH_2–10 wt% TiCN composite shows direct evidence of the improvement in the dehydrogenation kinetics resulted from the addition of TiCN.

The above results demonstrate that TiCN can both enhance desorption and absorption kinetics of MgH_2. However, the catalytic mechanism of MgH_2–10 wt% TiCN composite remains unknown. In order to shed light on the catalytic mechanism of TiCN, XRD patterns of bulk TiCN, ball-milled, dehydrogenated and rehydrogenated

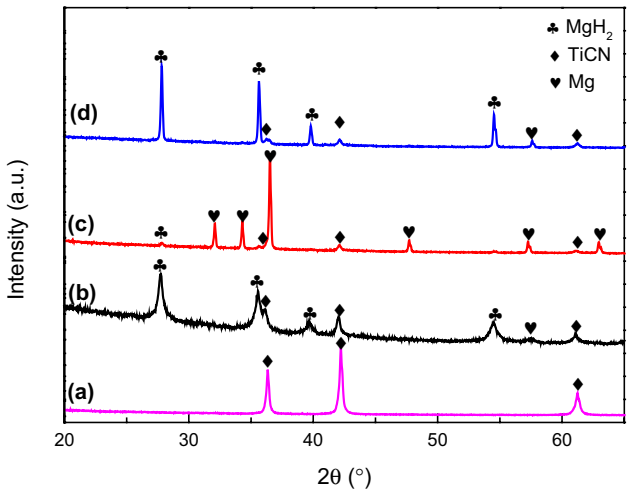

Fig. 7 The XRD patterns of (a) bulk TiCN, (b) ball-milled, (c) dehydrogenated and (d) rehydrogenated MgH_2–10 wt% TiCN samples

MgH_2–10 wt% TiCN samples are presented, shown in Fig. 7. It can be seen that all the four samples show the signal of TiCN phase and no diffraction signal pertinent to Ti/C/N phases or other Ti/C/N related compounds appear after

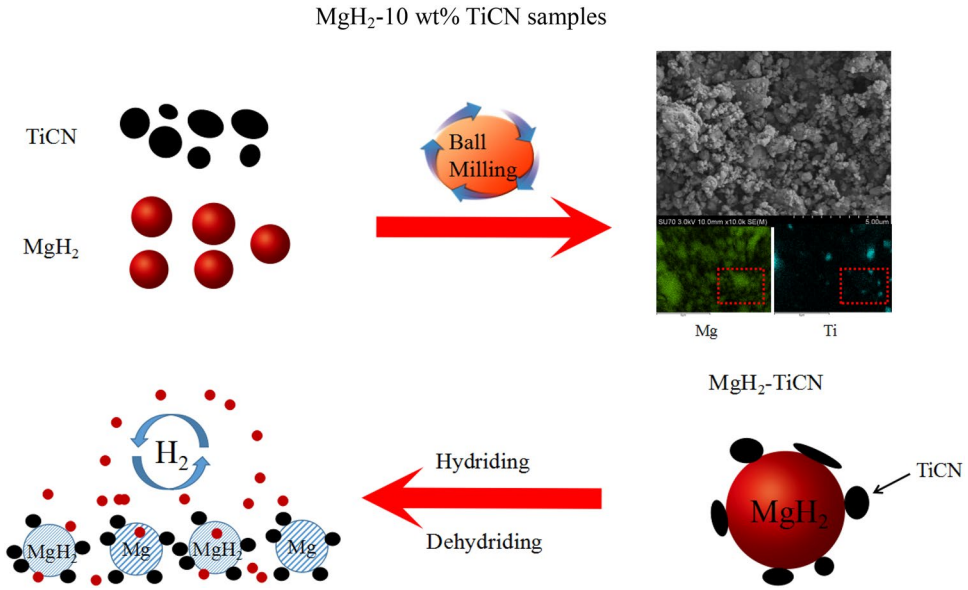

Fig. 8 The schematic illustration of synthesis and de/rehydrogenation process in MgH_2–TiCN composites

the de/rehydrogenation process, indicating that no evolution of the physical–chemical state of TiCN has occurred during the reversible hydrogen storage process. The XRD results provide direct evidence for the good stability of the doped TiCN, which serves as active specie in enhancing the hydrogen storage properties of MgH_2. Besides, the EDX mapping data in Fig. S2 shows that the small particles around MgH_2 were TiCN, demonstrating a uniform dispersion of TiCN, which may provide pathways for the hydrogen diffusion during de/rehydrogenation process, thus improving the hydrogen storage properties of MgH_2.

Based on the above analysis, Fig. 8 shows a schematic illustration of synthesis and de/rehydrogenation process of the MgH_2–TiCN composite. After ball milling, big TiCN particles were smashed to small ones, which were embedded in MgH_2. During the de/rehydrogenation cycles, the TiCN remained stable and acted as active specie, which not only acted as charge transfer between Mg/MgH_2 but also provided pathways for hydrogen diffusion, thus greatly improve the hydrogen de/rehydrogenation properties of MgH_2.

4 Conclusion

In summary, the MgH_2–x wt%TiCN ($x = 5$, 10, 15) composites prepared by ball milling and their microstructure and hydrogen storage properties were systematically investigated. Studies found that the de/rehydrogenation kinetics of MgH_2 can be significantly improved by the addition of TiCN. Considering the onset dehydrogenation temperature and isothermal de/rehydrogenation kinetics, the MgH_2–10 wt% TiCN composite showed the best performance. The MgH_2–10 wt% TiCN composite only needed 61.8, 17.3 and 8.5 min to release 4 wt% hydrogen at 275, 300 and 325 °C, respectively. However, as-synthesized MgH_2 did not release any H_2 at 275 °C and 300 °C. Besides, MgH_2–10 wt% TiCN composite could absorb 4.63 wt% H_2 under 3.2 MPa hydrogen pressure at 300 °C within 20 s. The activation energy of MgH_2–10 wt% TiCN was reduced to 106.82 ± 5 kJ/mol. XRD analysis demonstrated that the TiCN remains stable and acts as active catalytic specie during the de/rehydrogenation process. Based on the experimental results, a mechanism was proposed to illustrate how the TiCN acted as charge transfer between Mg/MgH_2 and H_2, consequently enhancing the de/rehydrogenation properties of MgH_2–TiCN composite.

Funding This study was funded by National Natural Science Foundation of China (Grant Nos. 51801078 and 51702300) and the National Science Foundation of Jiangsu Province (Grant Nos. BK20180986, 17KJB480003 and SJCX18-0772).

Compliance with ethical standards

Conflict of interest The authors declare that they have no conflict of interest.

References

1. Tena DLD, Pregger T (2018) Impact of electric vehicles on a future renewable energy-based power system in Europe with a focus on Germany. Int J Energy Res 42:2670–2685
2. Sigurjonsson HAE, Clausen LR (2018) Solution for the future smart energy system: a polygeneration plant based on reversible solid oxide cells and biomass gasification producing either electrofuel or power. Appl Energy 216:323–337

3. Züttel A, Callini E, Kato S, Atakli ZOK (2015) Storing renewable energy in the hydrogen cycle. Chimia 69:741–745
4. Wang Y, Wang Y (2017) Recent advances in additive-enhanced magnesium hydride for hydrogen storage. Progr Nat Sci Mater Int 27:41–49
5. Yu X, Tang Z, Sun D, Ouyang L, Zhu M (2017) Recent advances and remaining challenges of nanostructured materials for hydrogen storage applications. Prog Mater Sci 88:1–48
6. Liu H, Wang X, Liu Y, Dong Z, Cao G, Li S, Yan M (2013) Improved hydrogen storage properties of MgH_2 by ball milling with AlH_3: preparations, de/rehydriding properties, and reaction mechanisms. J Mater Chem A 1:12527–12535
7. Liu H, Wu C, Zhou H, Chen T, Liu Y, Wang X, Dong Z, Ge H, Li S, Yan M (2015) Synergistically thermodynamic and kinetic tailoring of the hydrogen desorption properties of MgH_2 by Co-Addition of AlH_3 and CeF_3. Rsc Adv 5:22091–22096
8. Kobayashi T, Takasaki A (2013) Ab initio study of the role of niobium oxides as catalysts in magnesium hydride. J Alloy Compd 580:S229–S232
9. Chen G, Zhang Y, Chen J, Guo X, Zhu Y, Li L (2018) Enhancing hydrogen storage performances of MgH_2 by Ni nano-particles over mesoporous carbon CMK-3. Nanotechnology 29:265705
10. Kumar S, Jain A, Miyaoka H, Ichikawa T, Kojima Y (2017) Catalytic effect of bis (cyclopentadienyl) nickel II on the improvement of the hydrogenation–dehydrogenation of Mg–MgH_2 system. Int J Hydrogen Energy 42:17178–17183
11. Jia Y, Yao X (2017) Carbon scaffold modified by metal (Ni) or non-metal (N) to enhance hydrogen storage of MgH_2 through nanoconfinement. Int J Hydrogen Energy 42:22933–22941
12. Yuan J, Zhu Y, Li Y, Zhang L, Li L (2014) Effect of multi-wall carbon nanotubes supported palladium addition on hydrogen storage properties of magnesium hydride. Int J Hydrogen Energy 39:10184–10194
13. Youn JS, Phan DT, Park CM, Jeon K (2017) Enhancement of hydrogen sorption properties of MgH_2 with a MgF_2 catalyst. Int J Hydrogen Energy 42:20120–20124
14. Cheng Y, Zhang W, Liu J, Cheng K, Zhao Z (2017) Effect of the nanometric $LiFePO_4$ on the hydrogen storage properties of MgH_2. Int J Hydrogen Energy 42:356–365
15. Chen J, Xia G, Guo Z, Huang Z, Liub H, Yu X (2015) Porous Ni nanofibers with enhanced catalytic effect on the hydrogen storage performance of MgH_2. J Mater Chem A 3:15843–15848
16. Sulaiman NNI, Ismail M (2016) Enhanced hydrogen storage properties of MgH_2 co-catalyzed with K_2NiF_6 and CNTs. Dalton Trans 45:19380–19388
17. Valentoni A, Mulas G, Enzo S, Garroni S (2018) Remarkable hydrogen storage properties of MgH_2 doped with $VNbO_5$. Phys Chem Chem Phys 20:4100–4108
18. Yahya M, Sulaiman N, Mustafa N, Halim Yap F, Ismail M (2018) Improvement of hydrogen storage properties in MgH_2 catalysed by K_2NbF_7. Int J Hydrogen Energy 43:14532–14540
19. Ali N, Idris N, Din M, Mustafa N, Sazelee N, Yap F, Sulaiman N, Yahya M, Ismail M (2018) Nanolayer-like-shaped $MgFe_2O_4$ synthesised via a simple hydrothermal method and its catalytic effect on the hydrogen storage properties of MgH_2. RSC Adv 8:15667–15674
20. Ma LP, Wang P, Cheng HM (2010) Hydrogen sorption kinetics of MgH_2 catalyzed with titanium compounds. Int J Hydrogen Energy 35:3046–3050
21. Wang Y, Zhang Q, Wang Y, Jiao L, Yuan H (2015) Catalytic effects of different Ti-based materials on dehydrogenation performances of MgH_2. J Alloy Compd 645:S509–S512
22. Hou X, Hu R, Yang Y, Feng L (2017) Isothermal activation, thermodynamic and hysteresis of MgH_2 hydrides catalytically modified by high-energy ball milling with MWCNTs and TiF_3. Int J Hydrogen Energy 42:22953–22964
23. Brum MC, Jardim PM, Santos DSD, Conceicao DMOT (2013) The effect of TTNT nanotubes on hydrogen sorption using MgH_2. Mater Res 16:647–649
24. Zhang Y, Zhuang X, Zhu Y, Wan N, Li L, Dong J (2015) Synergistic effects of TiH_2 and Pd on hydrogen desorption performances of MgH_2. Int J Hydrogen Energy 40:16338–16346
25. Su W, Zhu Y, Zhang J, Liu Y, Yang Y, Mao Q, Li L (2016) Effect of multi-wall carbon nanotubes supported nano-nickel and TiF_3 addition on hydrogen storage properties of magnesium hydride. J Alloy Compd 669:8–18
26. Kumar S, Kojima Y, Dey GK (2017) Tailoring the hydrogen absorption desorption's dynamics of Mg MgH_2 system by titanium suboxide doping. Int J Hydrogen Energy 42:21841–21848
27. Zhang X, Leng Z, Gao M, Hu J, Du F, Yao J, Pan H, Liu Y (2018) Enhanced hydrogen storage properties of MgH_2 catalyzed with carbon supported nanocrystalline TiO_2. J Power Sources 398:183–192
28. Ma LP, Wang P, Cheng HM (2007) Improving hydrogen sorption kinetics of MgH_2 by mechanical milling with TiF_3. J Alloy Compd 432:L1–L4
29. Pandey SK, Bhatnagar A, Shahi RR, Hudson MSL, Singh MK, Srivastava ON (2013) Effect of TiO_2 nanoparticles on the hydrogen sorption characteristics of magnesium hydride. J Nanosci Nanotechnol 13:5493–5499
30. Cui J, Wang H, Liu J, Ouyang L, Zhang Q, Sun D, Yao X, Zhu M (2013) Remarkable enhancement in dehydrogenation of MgH_2 by a nano-coating of multi-valence Ti-based catalysts. J Mater Chem A 1:5603–5611
31. Pitt MP, Paskevicius M, Webb CJ, Sheppard DA, Buckley CE, Gray EM (2012) The synthesis of nanoscopic Ti based alloys and their effects on the MgH_2 system compared with the MgH_2 +0.01Nb_2O_5 benchmark. Int J Hydrogen Energy 37:4227–4237
32. Liu Y, Du H, Zhang X, Yang Y, Gao M, Pan H (2015) Superior catalytic activity derived from a two-dimensional Ti_3C_2 precursor towards the hydrogen storage reaction of magnesium hydride. Chem Commun 52:705–708
33. El-Eskandarany MS, Shaban E, Alsairafi AA (2016) Synergistic dosing effect of TiC/FeCr nanocatalysts on the hydrogenation/dehydrogenation kinetics of nanocrystalline MgH_2 powders. Energy 104:158–170
34. Shin JH, Lee GJ, Cho YW, Lee KS (2009) Improvement of hydrogen sorption properties of MgH_2 with various sizes and stoichiometric compositions of TiC. Catal Today 146:209–215
35. Fan MQ, Liu SS, Zhang Y, Zhang J, Sun L, Xu F (2010) Superior hydrogen storage properties of MgH_2–10 wt% TiC composite. Energy 35:3417–3421
36. Wang Y, Li L, An C, Wang Y, Chen C, Jiao L, Yuan H (2014) Facile synthesis of TiN decorated graphene and its enhanced catalytic effects on dehydrogenation performance of magnesium hydride. Nanoscale 6:6684–6691
37. Gao S, Liu H, Xu L, Li S, Wang X, Yan M (2017) Hydrogen storage properties of nano-CoB/CNTs catalyzed MgH_2. J Alloy Compd 735:635–642
38. Milosevic S, Kurko S, Pasquini L, Matovic L, Vujasin R, Novakovic N, Novakovic JG (2016) Fast hydrogen sorption from MgH_2–VO_2(B) composite materials. J Power Sources 307:481–488
39. Zhang L, Chen L, Fan X, Xiao X, Zheng J, Huang X (2017) Enhanced hydrogen storage properties of MgH_2 with numerous hydrogen diffusion channels provided by $Na_2Ti_3O_7$ nanotubes. J Mater Chem A 5:6178–6185
40. Chuang YS, Hwang SJ (2016) Synthesis and hydrogen absorption/desorption properties of Mg–Nb_2O_5–SWCNT/MWCNT nanocomposite prepared by reactive milling. J Alloy Compd 656:835–842

41. Yahya M, Ismail M (2019) Catalytic effect of $SrTiO_3$ on the hydrogen storage behaviour of MgH_2. J Energy Chem 28:46–53
42. Mustafa NS, Sulaiman NN, Ismail M (2016) Effect of $SrFe_{12}O_{19}$ nanopowder on the hydrogen sorption properties of MgH_2. RSC Adv 6:110004–110010
43. Ismail M, Mustafa NS, Juahir N, Yap F (2016) Catalytic effect of $CeCl_3$ on the hydrogen storage properties of MgH_2. Mater Chem Phys 170:77–82